HHS Public Access

Author manuscript

Am J Ophthalmol. Author manuscript; available in PMC 2016 October 01.

Published in final edited form as:

Am J Ophthalmol. 2015 October ; 160(4): 786–98.e4. doi:10.1016/j.ajo.2015.06.032.

Multimodal imaging of central retinal disease progression in a 2 year mean follow up of Retinitis Pigmentosa

Tharikarn Sujirakul[1,2], **Michael K. Lin**[3], **Jimmy Duong**[4], **Ying Wei**[4], **Sara Lopez-Pintado**[4], and **Stephen H. Tsang**[1,5]

[1]Bernard & Shirlee Brown Glaucoma Laboratory and Barbara & Donald Jonas Stem Cell Laboratory, Department of Ophthalmology, Columbia University, New York, NY, USA [2]Department of Ophthalmology, Ramathibodi Hospital, Mahidol University, Bangkok, Thailand [3]College of Physicians & Surgeons, Columbia University, New York, NY, USA [4]Department of Biostatistics, Columbia University, New York, NY, USA [5]Department of Pathology and Cell Biology and Institute of Human Nutrition, Columbia University, New York, NY, USA

Abstract

Purpose—To determine the rate of progression and optimal follow up time in patients with advanced stage retinitis pigmentosa (RP) comparing the use of fundus autofluorescence imaging and spectral domain optical coherence tomography.

Design—Retrospective analysis of progression rate.

Methods—Longitudinal imaging follow up in 71 patients with retinitis pigmentosa was studied using the main outcome measurements of hyperautofluoresent ring horizontal diameter and vertical diameter along with ellipsoid zone line width from spectral domain optical coherence tomography. Test-retest reliability and the rate of progression were calculated. The interaction between the progression rates was tested for sex, age, mode of inheritance, and baseline measurement size. Symmetry of left and right eye progression rate was also tested.

Results—Significant progression was observed in >75% of patients during the 2 year mean follow up. The mean annual progression rates of ellipsoid zone line, and hyperautofluorescent ring horizontal diameter and vertical diameter were 0.45° (4.9%), 0.51° (4.1%), and 0.42° (4.0%), respectively. The e llipsoid zone line width, and hyperautofluorescent ring horizontal diameter and vertical diameter had low test-retest variabilities of 8.9%, 9.5% and 9.6%, respectively. This study is the first to demonstrate asymmetrical structural progression rate between right and left eye, which was found in 19% of patients. The rate of progression was significantly slower as the disease approached the fovea, supporting the theory that RP progresses in an exponential fashion.

Corresponding author: Stephen H. Tsang, M.D., Ph.D. Department of Ophthalmology, Edward S. Harkness Eye Institute, Columbia University, New York, NY, USA Tel: 1-212-342-1186, sht2@columbia.edu.

Supplemental Material available at AJO.com

No significant interaction between progression rate and patient age, sex, or mode of inheritance was observed.

Conclusions—Fundus autofluorescence and optical coherence tomography detect progression in patients with RP reliably and with strong correlation. These parameters may be useful alongside functional assessments as the outcome measurements for future therapeutic trials. Follow-up at 1 year intervals should be adequate to efficiently detect progression.

INTRODUCTION

Retinitis pigmentosa (RP) is characterized by a slow, progressive loss of photoreceptors primarily involving rods, followed by loss of cone photoreceptors. Early RP impairs night and peripheral vision, leaving central vision intact until later in the disease.[1]

The natural history of the disease has long been studied using functional measures such as visual acuity, visual field, and electrophysiology, which have provided substantial insight into the various patterns of disease progression. Visual field analyses revealed that aside from the basic pattern of concentric visual field loss, some patients exhibit scotomas in mid-peripheral regions of the visual field and some exhibit asymmetric visual field loss, though in the end stage of all patterns a central visual field remains with occasional small islands of peripheral vision.[2–4] While visual field and conventional visual function testing most closely capture the patient's perception of visual impairment, these tests are inherently subjective and have high test-retest variability.[5–7] The advent of full field electroretinography (ffERG) allowed for an objective, functional measurement of the retina, which assists in diagnosing RP and in monitoring the long-term disease course for prognosis and treatment response.[1,8–13] The different types of ERG monitor local and broad measurements of retina function. Full-field ERG measures the entire retina, pattern ERG measures the central retina, and multifocal ERG measures the innermost 30° of the retina; these modes of ERG greatly improved the reproducibility of functional measurements compared to visual field testing.[6,14–16] One important limitation of these functional studies, however, is that they have not been able to reliably detect small progression, especially in end stage disease, due to the variability of the testing results.[3,5–7,9,12,17,18]

Noninvasive imaging techniques such as spectral domain optical coherence tomography (SD-OCT) and fundus autofluorescence (AF) use objective, structural measurements, which have been shown to be well-correlated with functional measures of disease.[19–24] A landmark study led by Graham Holder et al first reported the presence of hyperautofluorescent rings in patients with RP in 2003.[15] Subsequently, the utility of fundus autofluorescence to measure the progression of RP was demonstrated in several series of studies that showed the correlation between structural and functional measurements and the correlation between the diameter of the hyperautofluorescent ring on AF and the width of the ellipsoid zone line on SD-OCT.[15,16,20,22–32] OCT and AF measurements of advanced RP did not correlate with ffERG, which assesses nonselective global responses of the retina.[15,27] Interestingly, some patients that were shown by OCT to have structurally intact maculae exhibited reduced focal ERG responses, which may have been due to a structural change not detected by the OCT device or functional deficit preceding structural deficit.[33,34] In these cases structural

measurements did not correlate with functional measurements, suggesting the usefulness of a multimodal approach to monitoring progression in the central retina.

Compared to functional assessments, structural imaging modalities focus at the posterior pole of the retina and have lower test-retest variability, hence improved sensitivity to detect the progression of advanced stage disease in a shorter period of time.[6,20,31,35,36] Furthermore, these two imaging modalities are widely available, and they can be more child friendly than ERG, which is important for monitoring family members of patients with RP. Given these qualities, these imaging modalities may be useful for visualizing the natural course of disease in a slow progressing disease like RP, and they may need consideration as outcome measurements to supplement functional measurements in assessing the efficacy of upcoming gene therapy and other treatment trials in RP, in which patients are often enrolled at advanced stage disease.[20,31] Because SD-OCT and AF are limited to structural assessment of the posterior pole, full-field ERG remains important in advanced stage disease to measure any peripheral retinal function, and other functional assessments that focus at the posterior pole may be useful to more fully quantify impairment in advanced disease.[28]

Investigators conducting gene therapy and cell-based treatment trials in RP have the unique capability of using the fellow eye as a treatment control, assuming that disease progression is highly symmetric in the left and right eyes.[37–39] In recent studies from our group and others, a small proportion of the patients were observed to have baseline asymmetry using structural imaging techniques.[23,36,40] However, asymmetric disease progression has yet to be described in typical retinitis pigmentosa patients.

The purpose of this study is to compare OCT and autofluorescence in monitoring RP progression at the posterior pole, to identify their test-retest reliabilities, and to determine the optimal follow up time in advanced stage RP. The study also addresses whether asymmetry between structural progression in the left and right eyes exists, and whether the rate of structural progression is affected by age, sex, mode of inheritance, and stage of the disease.

METHODS

Subjects

This study adhered to the tenets of the Declaration of Helsinki and was approved by the Institutional Review Boards of the Edward Harkness Eye Institute and Columbia University. All subjects gave their consents. From a total of 864 patients with typical RP who have been followed up in the electrodiagnostics clinic at Columbia University's Harkness Eye Institute, 71 patients were selected according to the following criteria. Patients were included if they were monitored for at least two visits. Because our clinic is an international referral center for RP, after initial diagnosis was made for a large number of our patients, care was transferred back to the primary provider, and these patients did not return for a second visit. No cases of unilateral RP, X-linked RP in female patients, or paravenous RP were included in the study. Fundus autofluorescence (AF) imaging and spectral domain optical coherence tomography (SD-OCT) were used to evaluate structural disease progression and disease status at every time point. Patients with advanced RP who exhibited no visible ellipsoid zone

line and no visible hyperautofluorescent ring were excluded along with patients with poor image quality.

Diagnoses of RP were made based on clinical history, fundus examination, and full-field electroretinogram results. The majority of the 71 patients in the cohort carried a diagnosis of autosomal recessive RP (67.6%), followed by autosomal dominant (26.8%) and X-linked RP (5.6%). Syndromic RP accounted for 12.7% of the patients, and all were diagnosed with Usher syndrome. Patients were divided into 3 groups according to mode of inheritance (autosomal dominant, autosomal recessive, or X-linked), with the Usher syndrome patients included in the autosomal recessive subgroup.

Genetic Analyses

Blood was drawn from insured patients and DNA was extracted and tested on the published retinitis pigmentosa genes of the Chiang panel at Oregon Health Sciences University by parallel sequencing on Illumina HiSeq platform with 100 bp paired-end reads. Mutations were confirmed by dideoxy chain-terminating sequencing.

Image Acquisition

Fundus Autofluorescence (AF)—After pupil dilation, fundus autofluorescence (AF) imaging and spectral domain Optical Coherence Tomography (SD-OCT) was performed using the Spectralis HRA+OCT device (Heidelberg Engineering, Dossenheim, Germany) in each visit. AF imaging was acquired at a resolution of 1536x1536 pixels with a 30-degree field of view or if the ring was larger, a 55-degree field of view. The excitation wavelength was 488 nm. A 521 nm barrier filter was used to filter the emitted fluorescence light. The horizontal diameter and vertical diameter of the external boundary of the hyperautofluorescent ring were measured using the measuring tool provided in the Spectralis Software (Fig. 1). The external boundary is preferred over the internal boundary due to its more distinct appearance and its presence in a higher number of patients with RP, which allows greater precision to define the border. In cases involving a hyperautofluorescent arc rather than a complete ring, or a nasal edge of the ring that falls outside the optic nerve, only one axis was measured.

Spectral domain optical coherence tomography (SD-OCT)—SD-OCT images were acquired with an 870 nm light source, using an automatic real-time registration program from the Spectralis HRA+OCT device (Heidelberg Engineering, Dossenheim, Germany). Horizontal scan through the fovea was used to evaluate the width of the residual ellipsoid zone line using the measuring tool provided in the machine (Figure 1). Each studied parameter was measured twice by one observer.

STATISTICAL ANALYSIS

At each visit, fundus autofluorescence and SD-OCT were imaged. To assess test-retest reliability, from each studied image, two measurements were taken several weeks apart by first author TS for each parameter (ellipsoid zone line width, horizontal and vertical hyperautofluorescent ring diameter). The absolute difference between these two replicate measurements was calculated and summary statistics reported. In addition, the Bland

Altman method was used to calculate the coefficient of repeatability, defined as the 95th percentile of the difference between two methods of measurement.[41] For each structural imaging modality parameter, the intraclass correlation coefficient (ICC) was calculated to assess the reliability of test-retest measurements. Pearson correlation coefficient was used to examine the relationship between these three parameters, and the average of the two measurements for each parameter was used for this analysis. Progression rate was defined as a reduction in size of the parameter greater than the threshold for significant change, set at the 75th percentile of test-retest measurements. The proportion of patients that would have progressed at incremental follow up times was estimated by projecting the best fit line–described below—for each patient to determine if the decline would be greater than the threshold for significant change.

To model the trajectories of each of the variables measured from structural imaging modalities, linear mixed models were fit. The outcomes for these different models were ellipsoid zone line width, horizontal ring diameter, and vertical ring diameter. All linear mixed models included random intercepts and random slopes for subjects over time. The random slopes estimated the change over time for each subject. Left and right eyes were modeled separately. Variability between left and right eye measurements was tested and no significant difference was observed (data not shown). For presentation purposes, only the right eye was selected to represent the natural rate of progression. We examined the hypothesis of whether the right and left eyes of a patient progress similarly. For each subject, the difference in progression rate between the left and right eyes was calculated. This difference was compared to the variability of progression rate due to measurement error, which was calculated from test-retest observations of the right eye.

To examine whether the progression rate varied by another factor, linear mixed models were fit which included time and the factor in question, using an interaction between time and the potential factor as predictors. The other factors examined were age, sex, mode of inheritance, and stage of disease. All statistical analysis was performed using R version 3.1.0.

RESULTS

Clinical data

A total of 71 patients were analyzed in this study. 19 patients (26.8%) had ADRP, 48 (67.6%) had ARRP, and 4 (5.6%) had XLRP. 32 (45.1%) were female and 39 (54.9%) were male. The average age of patients at the initial visit was 40.4 ± 19.4 (range 12–81) years. The average follow up time was 2.1 (range 0.3–7.7) years, and the frequency of follow up ranged from 2–6 visits during the follow up time. Patients' clinical and genetic details are summarized in Table 1. Regarding the patients' retinal imaging phenotypes, 69 (97.2%) of the patients had an ellipsoid zone within the SD-OCT field of view, 48 (67.6%) had both an ellipsoid zone and a hyperautofluorescent ring and of the 2 patients with ellipsoid zones that extended outside the SD-OCT field of view, both had a measureable hyperautofluorescent ring. Different autofluorescence patterns were found as expected. 49 (69.0%) patients had a hyperautofluorescent ring, 17 (23.9 %) had central patchy hyperautofluorescence and 5

(7.0%) had no abnormal hyperautofluorescent pattern. 11 (15%) of the patients included in this study were observed to have cystoid macular edema (CME).

Reliability of the three measurements

Test-retest measurements were analyzed by descriptive statistics, the Bland Altman method, and intraclass correlation. The upper quartile of the difference between test and retest measurements was 112.5μm for ellipsoid zone width, 116.0μm for horizontal diameter, and 110.8μm for vertical diameter. Other descriptive statistics are reported in Table 2. The Bland Altman method was used to determine the coefficient of repeatability—with percentage of the mean initial measurement in parentheses— calculated to be 233.2μm (8.9%) for ellipsoid zone width, 312.1μm (8.5%) for horizontal diameter, and 291.2μm (9.6%) for vertical diameter. Intraclass correlation (ICC) of each of the three measurement parameters also showed high test-retest reliability (ICC = 0.999 for ellipsoid zone width, ICC = 0.997 for horizontal diameter and ICC = 0.997 for vertical diameter).

Next, we assessed the relationship between the three imaging parameters ellipsoid zone line, horizontal ring diameter, and vertical ring diameter. Pearson's correlation revealed a strong relationship between the 3 parameters; (Figure 2) r= 0.97 for ellipsoid zone line and horizontal diameter measurements, r= 0.96 for ellipsoid zone line and vertical diameter measurements, and r=0.97 for horizontal diameter and vertical diameter measurements.

Proportion of eyes showing progression

For each of the three parameters, the 75th percentile of the test-retest measurement variability was used as the threshold for significant change (table 2). Over the follow up period, ellipsoid zone line measurements showed 54/67 (81%) patients having significant change while horizontal diameter measurements showed 33/42 (79%) patients and vertical diameter measurements showed 35/45 (78%) patients with significant change. The change over time for each subject was estimated from linear mixed models. To project the number of patients who would have shown structural disease progression during incremental lengths of follow up, the 75th percentile of the test retest measurement variability was again used as the threshold for significant change, and by 1.5 years of follow up over 50% of the patients were projected to have significantly progressed using each of the three measurement parameters (table 3).

Rate of Progression

The estimated mean shortening of the ellipsoid zone line was 130 μm (0.45°)/year (se=11, p-value <0.001). Using the hyperautofluorescent ring, the estimated mean constriction of horizontal diameter was 147 μm (0.51°) /year (se=15, p-value <0.001), and the estimated mean constriction of vertical diameter was 121 μm (0.42°) /year (se=15, p-value <0.001). Represented as a decrease from the mean value of the initial visit, the cohort had a yearly progression rate of 4.9% by ellipsoid zone line, 4.1% by horizontal diameter, and 4.0% by vertical diameter.

Examining for interactions between time and other factors

To examine whether change over time for each of the outcomes varied by another factor, models were fit with interaction terms. Here, we considered possible interactions with age at baseline, sex, mode of inheritance, or size of the measurement at baseline (Supplemental Tables 1–4). A significant difference in rate of structural progression was only observed when comparing the size of the hyperautofluorescent ring or the ellipsoid zone line when patients were grouped by baseline size (<3000 μm and ≥3000 μm). See Table 3 and Supplemental Table 4. Larger measurements at baseline tended to have a faster rate of progression, and differences in mean rates of progression between those patients with baseline measurements <3000 μm vs. ≥3000 μm ranged from 20 to 110 μm/year. For ellipsoid zone line and vertical diameter, these differences had p-values <0.05 for both right and left eyes. For horizontal diameter, these differences were not statistically significant.

Differential rate of decline between left and right eye

Asymmetry between left and right eye disease severity is sometimes seen at baseline,[36] and we have observed asymmetry in progression during clinical followup using structural assessments (Figure 4). Hence, to assess the proportion of asymmetry between progression rate in the left and right eye, the difference between left and right eye progression rates was compared against the variation of progression rates calculated using test-retest measurements of the right eye. In ellipsoid zone line measurements, the variability of absolute differences between left and right eye (standard deviation of 62 μm) was higher than the variability of differences from test-retest measurements of the right eye (standard deviation of 43 μm), suggesting that left and right eye progress differently. To determine the number of patients with significant difference in left and right eye structural progression, the threshold of significant difference between left and right eye was set to be 94.1 μm/year, which is the 95th percentile of the difference of ellipsoid zone line progression rates calculated from the test and retest of the right eye of each patient. Applying this threshold, we observed that 19% (12/63) of our patients had asymmetry in the structural progression rate between the two eyes. The same analysis on hyperautofluorescent ring diameters showed no evidence of a difference between progression rate in left and right eyes.

DISCUSSION

This study demonstrates that structural measurements of disease progression using ellipsoid zone line width from SD-OCT and hyperautofluorescent ring diameter from AF are reliable and can detect progression for advanced stage RP. From our study, the group mean rate of structural progression for advanced stage disease was approximately 0.5° per year. Using these parameters , a mean follow up period of two years was sufficient to detect structural disease progression. Approximately 20% of patients manifested a different rate of structural progression between left and right eye, so investigators need to be aware of this possibility when designing and interpreting interventional trials.

Our study demonstrated that the measurements from each of the three parameters, horizontal diameter and vertical diameter of the hyperautofluorescent ring and ellipsoid zone line width of SD-OCT are reliable and well-correlated to each other, similar to what was observed in

previous studies.[20,24,28,29,31,36] The ellipsoid zone line was able to follow up patients until the end stage of the disease, but a major limitation of the ellipsoid zone line is that because the field is limited to 30° by the SD-OCT device, the disease can only be monitored when it has already reached the posterior pole, and hence we were unable to monitor 2 (2.8%) of the patients in our study. [31] An advantage of AF is the capacity to image a wider field that allows assessment of patients with earlier stage disease, though future OCT devices such as swept-source OCT will also provide a wider view. As the disease progresses to end stage, hyperautofluorescent ring constriction results in central patchy hyperautofluorescence and atrophy, which is no longer measureable by AF, but the remaining photoreceptors can still be monitored by OCT. [23,27,42] Furthermore, a small percentage (7%) of our patients with RP presented with speckled, granulated, and fractured ellipsoid zones for which we were unable to determine the width of the ellipsoid zone line, but we were able to detect a distinct hyperautofluorescent ring. In addition, our study had relatively few patients with CME (15%), which was because patients with CME often had distorted retinal layers which made accurate visualization of the ellipsoid zone line and the hyperautofluorescent ring difficult, and hence, many patients with CME were excluded.[43] Another contributing factor to the low number of patients with CME in our cohort was that we did not regard small single cystic changes without foveal involvement or macular or retinal edema to be significant CME.

The rate of progression and natural course of retinitis pigmentosa has been studied using functional and structural assessment modalities. Functional assessment is more related to useful vision and directly represents the quality of life of the patients compared to objective assessment. Full field ERG is considered to be the most important tool in assessing progression in RP,[10] and other functional tests play a subsidiary role. However, functional assessments have been reported to have large test-retest variability; 20–40% in visual field, and 10–20% in multifocal ERG.[6,35] Several functional tests rely on subjective patient responses, but even with objective functional assessments such as full field ERG, the variability is still high in normal subjects (at least 25%) and similar in affected individuals.[44,45] While ERG is adequate for measuring long-term progression in patients with RP, the test-retest variability of ERG measurements makes it challenging to assess the slow progression of RP over short followup periods. Also because full field ERG measures the entire retina, it is less suitable in the advanced stage of RP when the macula is the only part of the retina remaining.[17] In this study we have shown that variability in structural measures using OCT and AF are 8.9% for ellipsoid zone width, 8.5% for horizontal ring diameter, and 9.6% for vertical ring diameter, which are substantially lower than the previously reported ERG values. The variability of 8.9% for ellipsoid zone width in our study is slightly higher than the variability of 3.6% previously reported in an XLRP study.[20]

We were able to detect structural progression in 80.6% of the patients in our cohort using the ellipsoid zone line, 78.6% using the hyperautofluorescent ring horizontal diameter, and 77.8% using the hyperautofluorescent ring vertical diameter during the follow up period. Due to the lower variability of these 3 parameters, they markedly lowered the threshold to detect significant change in disease progression in advanced stage disease compared to that of functional tests.[6,35,44] From our study by using these parameters, a 1.5 year follow up period was projected to detect structural progression at the posterior pole in the majority of patients with RP, which is similar to what was reported in other studies of AF and OCT,[20,40]

and which is a shorter time compared to functional assessments such as full-field ERG that may require 3–4 years to detect progression.[8,17] For phase II or III efficacy trials in which the ideal test would have the highest sensitivity in detecting progression over a short followup period in advanced stage disease, using objective, structural assessment may be a useful additional approach that may shorten the duration needed for outcome measurements in future therapeutic trials.[2,17,23,30]. The phase I/II gene therapy studies in early onset retinal dystrophy used OCT and AF as outcome measurements to monitor safety and efficacy along with functional assessments.[46–48] In addition, OCT has been used to supplement functional assessments of disease progression in stem cell and neutrophic factor interventional trials.[49,50]

In this study, the mean annual decrease in ellipsoid zone line width was 130 μm (4.9%)and the constriction rates of horizontal ring diameter and vertical ring diameter were 147 μm (4.1%)and 121 μm (4.0 %), which is comparable with previous studies on progression with both functional and structural assessments, ERG 8.7–18.5%[8,10,17], visual field 2.6–14.5%[2,3,11,51,52], multifocal ERG 6–10%[52], AF ring constriction 0.8–15%[23,27,30], and ellipsoid zone line 7–10.9%.[20,30]

Our study observed no difference in rates of structural progression by age or by sex. This is consistent with previous studies, and this could be the result of selection bias because only children with severe disease would be diagnosed while those with mild disease would remain undiagnosed.[27] Although XLRP is more severe and has faster rate of progression compared to other genetic modes,[17,18,20] we could not find a statistically significant difference between the mode of inheritance and the rate of structural progression. However, we have only 4 patients in XLRP group, so the lack of a difference is likely due to the small sample size.

We observed a significantly lower mean rate of structural progression in patients with measurements <3000μm compared to >3000μm, which indicates the progression rate decreases as the disease approaches the fovea. This finding was statistically significant in previous functional studies,[52,53] and observationally the same trend was reported in other functional and structural studies.[10,13,20,23] This data provides evidence supporting the theory that retinitis pigmentosa progresses in 1st order rate with exponential decay shown in animal models with various gene defects.[54] However, in this study the overall progression was best fit with linear trend because the follow up time was relatively short with few measurement points. Furthermore, many of our patients presented in advanced stage disease, and the progression may have reached a plateau at the time of presentation, unlike in mouse models for which we can study progression from the initiation of the disease.

RP has been assumed to be bilateral and highly symmetric due to its genetic etiology.[39] Hence, most previous studies average the measurements between the eyes for analysis. Despite the assumed symmetry in RP, a small number of patients with asymmetric and unilateral RP have been reported.[23,55] A genetic confirmation has not been shown for unilateral RP except for one case of a patient with an RP1 mutation.[56] Our previous study using hyperautofluorescent ring measurements showed 12.7–14.3% of patients with RP present with asymmetrical ring size, which was similar to the 10% of patients reported from

an Usher Syndrome natural progression study.[23,36] Another study using AF and SD-OCT to monitor RP progression also found asymmetry between eyes with no significant correlation between the left and right eye.[40] In the present study, we observed approximately 20% of our patients had a significant difference in structural progression rate at the posterior pole between left and right eyes. Of the three measurement parameters, only ellipsoid zone line measurements were able to detect asymmetric progression. From this, we infer that the asymmetry of the left and right eye progression rates at the posterior pole is subtle, and more patients may need to be followed to statistically demonstrate whether asymmetric structural progression occurs for hyperautofluorescent ring measurements. Further studies with extended followup are needed to determine whether the asymmetry is present throughout the disease course, whether there are any correlations of the asymmetry to functional tests and whether CME, inflammation, or other clinical findings are possible underlying factors. Treatment trials using the fellow eye as a control need to be interpreted with caution given the possibility of asymmetric progression.

This study demonstrates that imaging using SD-OCT and fundus autofluorescence are effective in monitoring structural RP progression in advanced stage disease. The hyperautofluorescent ring from AF and the ellipsoid zone line width from OCT complement each other in detecting structural disease progression at the posterior pole, so they may be useful to supplement functional measures ERG and visual field in routine monitoring of disease progression in patients with advanced disease. These structural parameters may also be considered alongside functional assessments as outcome measurements for future therapeutic trials. Studies of longer duration and more patient enrollment are needed to expand upon the results generated from this study to improve RP monitoring using imaging techniques, to demonstrate whether functional correlations exist, and to determine what underlying factors contribute to the observed asymmetric structural progression.

Supplementary Material

Refer to Web version on PubMed Central for supplementary material.

Acknowledgments

Tharikarn Sujirakul was supported by Foundation Fighting Blindness, Owings Mills, Maryland grant CF-CL-0613-0614-COLU. The Barbara & Donald Jonas Laboratory is supported by National Institute of Health, Bethesda, Maryland, Core grant 5P30EY019007; National Cancer Institute, Bethesda, Maryland, Core grant 5P30CA013696; and unrestricted funds from Research to Prevent Blindness, Columbia University, New York. S.H.T. is a member of the RD-CURE Consortium, Tubingen, Germany, and is supported by New York State Stem Cell Science, New York, New York, grants N09G-302 and N13G-275; the Foundation Fighting Blindness, Owings Mills, Maryland, New York Regional Research Center Grant (C-NY05-0705-0312); the National Eye Institute, Bethesda, Maryland, grant R01EY018213 and R21AG050437; the Research to Prevent Blindness Physician-Scientist Award, the Schneeweiss Stem Cell Fund, Tistou and Charlotte Kerstan Foundation, Joel Hoffman Fund, Gale and Richard Siegel Stem Cell Fund, Charles Culpeper Scholarship, Laszlo Bito and Olivia Carino Foundation, Professor Gertrude Rothschild Stem Cell Foundation, and Gebroe Family Foundation – all based in New York, New York. The authors are grateful to the members of the photography department at the Edward S. Harkness Eye Institute, Columbia University, New York, New York, for their assistance in obtaining images for this article.

References

1. Hartong DT, Berson EL, Dryja TP. Retinitis pigmentosa. Lancet. Nov 18; 2006 368(9549):1795–1809. [PubMed: 17113430]

2. Fishman GA, Bozbeyoglu S, Massof RW, Kimberling W. Natural course of visual field loss in patients with Type 2 Usher syndrome. Retina. Jun; 2007 27(5):601–608. [PubMed: 17558323]
3. Grover S, Fishman GA, Anderson RJ, Alexander KR, Derlacki DJ. Rate of visual field loss in retinitis pigmentosa. Ophthalmology. Mar; 1997 104(3):460–465. [PubMed: 9082273]
4. Grover S, Fishman GA, Brown J Jr. Patterns of visual field progression in patients with retinitis pigmentosa. Ophthalmology. Jun; 1998 105(6):1069–1075. [PubMed: 9627658]
5. Holopigian K, Greenstein V, Seiple W, Carr RE. Rates of change differ among measures of visual function in patients with retinitis pigmentosa. Ophthalmology. Mar; 1996 103(3):398–405. [PubMed: 8600415]
6. Seiple W, Clemens CJ, Greenstein VC, Carr RE, Holopigian K. Test-retest reliability of the multifocal electroretinogram and humphrey visual fields in patients with retinitis pigmentosa. Doc Ophthalmol. Nov; 2004 109(3):255–272. [PubMed: 15957611]
7. Madreperla SA, Palmer RW, Massof RW, Finkelstein D. Visual acuity loss in retinitis pigmentosa. Relationship to visual field loss. Arch Ophthalmol. Mar; 1990 108(3):358–361. [PubMed: 2310334]
8. Berson EL, Sandberg MA, Rosner B, Birch DG, Hanson AH. Natural course of retinitis pigmentosa over a three-year interval. Am J Ophthalmol. Mar 15; 1985 99(3):240–251. [PubMed: 3976802]
9. Berson EL, Rosner B, Sandberg MA, et al. Vitamin A supplementation for retinitis pigmentosa. Arch Ophthalmol. Nov; 1993 111(11):1456–1459. [PubMed: 8240091]
10. Berson EL, Rosner B, Sandberg MA, et al. A randomized trial of vitamin A and vitamin E supplementation for retinitis pigmentosa. Arch Ophthalmol. Jun; 1993 111(6):761–772. [PubMed: 8512476]
11. Berson EL, Rosner B, Weigel-DiFranco C, Dryja TP, Sandberg MA. Disease progression in patients with dominant retinitis pigmentosa and rhodopsin mutations. Invest Ophthalmol Vis Sci. Sep; 2002 43(9):3027–3036. [PubMed: 12202526]
12. Berson EL, Rosner B, Sandberg MA, et al. Clinical trial of docosahexaenoic acid in patients with retinitis pigmentosa receiving vitamin A treatment. Arch Ophthalmol. Sep; 2004 122(9):1297–1305. [PubMed: 15364708]
13. Berson EL, Rosner B, Sandberg MA, et al. Further evaluation of docosahexaenoic acid in patients with retinitis pigmentosa receiving vitamin A treatment: subgroup analyses. Arch Ophthalmol. Sep; 2004 122(9):1306–1314. [PubMed: 15364709]
14. Seeliger M, Kretschmann U, Apfelstedt-Sylla E, Ruther K, Zrenner E. Multifocal electroretinography in retinitis pigmentosa. Am J Ophthalmol. Feb; 1998 125(2):214–226. [PubMed: 9467449]
15. Robson AG, El-Amir A, Bailey C, et al. Pattern ERG correlates of abnormal fundus autofluorescence in patients with retinitis pigmentosa and normal visual acuity. Invest Ophthalmol Vis Sci. Aug; 2003 44(8):3544–3550. [PubMed: 12882805]
16. Robson AG, Saihan Z, Jenkins SA, et al. Functional characterisation and serial imaging of abnormal fundus autofluorescence in patients with retinitis pigmentosa and normal visual acuity. Br J Ophthalmol. Apr; 2006 90(4):472–479. [PubMed: 16547330]
17. Birch DG, Anderson JL, Fish GE. Yearly rates of rod and cone functional loss in retinitis pigmentosa and cone-rod dystrophy. Ophthalmology. Feb; 1999 106(2):258–268. [PubMed: 9951474]
18. Hoffman DR, Locke KG, Wheaton DH, Fish GE, Spencer R, Birch DG. A randomized, placebo-controlled clinical trial of docosahexaenoic acid supplementation for Xlinked retinitis pigmentosa. Am J Ophthalmol. Apr; 2004 137(4):704–718. [PubMed: 15059710]
19. Robson AG, Egan CA, Luong VA, Bird AC, Holder GE, Fitzke FW. Comparison of fundus autofluorescence with photopic and scotopic fine-matrix mapping in patients with retinitis pigmentosa and normal visual acuity. Invest Ophthalmol Vis Sci. Nov; 2004 45(11):4119–4125. [PubMed: 15505064]
20. Birch DG, Locke KG, Wen Y, Locke KI, Hoffman DR, Hood DC. Spectral-domain optical coherence tomography measures of outer segment layer progression in patients with x-linked retinitis pigmentosa. JAMA Ophthalmol. Sep 1; 2013 131(9):1143–1150. [PubMed: 23828615]

21. Greenstein VC, Duncker T, Holopigian K, et al. Structural and functional changes associated with normal and abnormal fundus autofluorescence in patients with retinitis pigmentosa. Retina. Feb; 2012 32(2):349–357. [PubMed: 21909055]
22. Lenassi E, Troeger E, Wilke R, Hawlina M. Correlation between macular morphology and sensitivity in patients with retinitis pigmentosa and hyperautofluorescent ring. Invest Ophthalmol Vis Sci. Jan; 2012 53(1):47–52. [PubMed: 22110079]
23. Fakin A, Jarc-Vidmar M, Glavac D, Bonnet C, Petit C, Hawlina M. Fundus autofluorescence and optical coherence tomography in relation to visual function in Usher syndrome type 1 and 2. Vision Res. Dec 15.2012 75:60–70. [PubMed: 23000274]
24. Wakabayashi T, Sawa M, Gomi F, Tsujikawa M. Correlation of fundus autofluorescence with photoreceptor morphology and functional changes in eyes with retinitis pigmentosa. Acta Ophthalmol. Aug; 2010 88(5):e177–183. [PubMed: 20491687]
25. Popovic P, Jarc-Vidmar M, Hawlina M. Abnormal fundus autofluorescence in relation to retinal function in patients with retinitis pigmentosa. Graefes Arch Clin Exp Ophthalmol. Oct; 2005 243(10):1018–1027. [PubMed: 15906064]
26. Robson AG, Michaelides M, Saihan Z, et al. Functional characteristics of patients with retinal dystrophy that manifest abnormal parafoveal annuli of high density fundus autofluorescence; a review and update. Doc Ophthalmol. Mar; 2008 116(2):79–89. [PubMed: 17985165]
27. Robson AG, Tufail A, Fitzke F, et al. Serial imaging and structure-function correlates of high-density rings of fundus autofluorescence in retinitis pigmentosa. Retina. Sep; 2011 31(8):1670–1679. [PubMed: 21394059]
28. Robson AG, Lenassi E, Saihan Z, et al. Comparison of fundus autofluorescence with photopic and scotopic fine matrix mapping in patients with retinitis pigmentosa: 4- to 8-year follow-up. Invest Ophthalmol Vis Sci. 2012; 53(10):6187–6195. [PubMed: 22899761]
29. Lima LH, Cella W, Greenstein VC, et al. Structural assessment of hyperautofluorescent ring in patients with retinitis pigmentosa. Retina. Jul-Aug;2009 29(7):1025–1031. [PubMed: 19584660]
30. Lima LH, Burke T, Greenstein VC, et al. Progressive constriction of the hyperautofluorescent ring in retinitis pigmentosa. Am J Ophthalmol. Apr; 2012 153(4):718–727. 727 e711–712. [PubMed: 22137208]
31. Ramachandran R, Zhou L, Locke KG, Birch DG, Hood DC. A Comparison of Methods for Tracking Progression in X-Linked Retinitis Pigmentosa Using Frequency Domain OCT. Transl Vis Sci Technol. Nov.2013 2(7):5. [PubMed: 24349883]
32. Lenassi E, Saihan Z, Cipriani V, et al. Natural history and retinal structure in patients with Usher syndrome type 1 owing to MYO7A mutation. Ophthalmology. Feb; 2014 121(2):580–587. [PubMed: 24199935]
33. Moschos MM, Chatziralli IP, Verriopoulos G, Triglianos A, Ladas DS, Brouzas D. Correlation between optical coherence tomography and multifocal electroretinogram findings with visual acuity in retinitis pigmentosa. Clin Ophthalmol. 2013; 7:2073–2078. [PubMed: 24204109]
34. Sugita T, Kondo M, Piao CH, Ito Y, Terasaki H. Correlation between macular volume and focal macular electroretinogram in patients with retinitis pigmentosa. Invest Ophthalmol Vis Sci. Aug; 2008 49(8):3551–3558. [PubMed: 18441311]
35. Marmor MF. Do you, doctor, take the mfERG.for better or for worse? Graefes Arch Clin Exp Ophthalmol. Apr; 2002 240(4):241–243. [PubMed: 11981637]
36. Sujirakul T, Davis R, Erol D, et al. Bilateral Concordance of the Fundus Hyperautofluorescent Ring in Typical Retinitis Pigmentosa Patients. Ophthalmic Genet. Oct 10.2013
37. Testa F, Maguire AM, Rossi S, et al. Three-year follow-up after unilateral subretinal delivery of adeno-associated virus in patients with Leber congenital Amaurosis type 2. Ophthalmology. Jun; 2013 120(6):1283–1291. [PubMed: 23474247]
38. Bainbridge JW, Smith AJ, Barker SS, et al. Effect of gene therapy on visual function in Leber's congenital amaurosis. N Engl J Med. May 22; 2008 358(21):2231–2239. [PubMed: 18441371]
39. Massof RW, Finkelstein D, Starr SJ, Kenyon KR, Fleischman JA, Maumenee IH. Bilateral symmetry of vision disorders in typical retinitis pigmentosa. Br J Ophthalmol. Feb; 1979 63(2): 90–96. [PubMed: 311654]

40. Aizawa S, Mitamura Y, Hagiwara A, Sugawara T, Yamamoto S. Changes of fundus autofluorescence, photoreceptor inner and outer segment junction line, and visual function in patients with retinitis pigmentosa. Clin Experiment Ophthalmol. Aug; 2010 38(6):597–604. [PubMed: 20456441]
41. Bland JM, Altman DG. Statistical methods for assessing agreement between two methods of clinical measurement. Lancet. Feb 8; 1986 1(8476):307–310. [PubMed: 2868172]
42. Murakami T, Akimoto M, Ooto S, et al. Association between abnormal autofluorescence and photoreceptor disorganization in retinitis pigmentosa. Am J Ophthalmol. Apr; 2008 145(4):687–694. [PubMed: 18242574]
43. Adackapara CA, Sunness JS, Dibernardo CW, Melia BM, Dagnelie G. Prevalence of cystoid macular edema and stability in oct retinal thickness in eyes with retinitis pigmentosa during a 48-week lutein trial. Retina. Jan; 2008 28(1):103–110. [PubMed: 18185146]
44. Grover S, Fishman GA, Birch DG, Locke KG, Rosner B. Variability of full-field electroretinogram responses in subjects without diffuse photoreceptor cell disease. Ophthalmology. Jun; 2003 110(6):1159–1163. [PubMed: 12799241]
45. Fishman GA, Chappelow AV, Anderson RJ, Rotenstreich Y, Derlacki DJ. Short-term inter-visit variability of erg amplitudes in normal subjects and patients with retinitis pigmentosa. Retina. Dec; 2005 25(8):1014–1021. [PubMed: 16340532]
46. Jacobson SG, Cideciyan AV, Roman AJ, et al. Improvement and decline in vision with gene therapy in childhood blindness. N Engl J Med. May 14; 2015 372(20):1920–1926. [PubMed: 25936984]
47. Bainbridge JW, Mehat MS, Sundaram V, et al. Long-term effect of gene therapy on Leber's congenital amaurosis. N Engl J Med. May 14; 2015 372(20):1887–1897. [PubMed: 25938638]
48. Wright AF. Long-term effects of retinal gene therapy in childhood blindness. N Engl J Med. May 14; 2015 372(20):1954–1955. [PubMed: 25938534]
49. Pilli S, Zawadzki RJ, Telander DG. The dose-dependent macular thickness changes assessed by fd-oct in patients with retinitis pigmentosa treated with ciliary neurotrophic factor. Retina. Jul; 2014 34(7):1384–1390. [PubMed: 24368307]
50. Siqueira RC, Messias A, Voltarelli JC, Scott IU, Jorge R. Intravitreal injection of autologous bone marrow-derived mononuclear cells for hereditary retinal dystrophy: a phase I trial. Retina. Jun; 2011 31(6):1207–1214. [PubMed: 21293313]
51. Sandberg MA, Rosner B, Weigel-DiFranco C, McGee TL, Dryja TP, Berson EL. Disease course in patients with autosomal recessive retinitis pigmentosa due to the USH2A gene. Invest Ophthalmol Vis Sci. Dec; 2008 49(12):5532–5539. [PubMed: 18641288]
52. Nagy D, Schonfisch B, Zrenner E, Jagle H. Long-term follow-up of retinitis pigmentosa patients with multifocal electroretinography. Invest Ophthalmol Vis Sci. Oct; 2008 49(10):4664–4671. [PubMed: 18566474]
53. Iannaccone A, Kritchevsky SB, Ciccarelli ML, et al. Kinetics of visual field loss in Usher syndrome Type II. Invest Ophthalmol Vis Sci. Mar; 2004 45(3):784–792. [PubMed: 14985291]
54. Clarke G, Collins RA, Leavitt BR, et al. A one-hit model of cell death in inherited neuronal degenerations. Nature. Jul 13; 2000 406(6792):195–199. [PubMed: 10910361]
55. Marsiglia M, Duncker T, Peiretti E, Brodie SE, Tsang SH. Unilateral retinitis pigmentosa: a proposal of genetic pathogenic mechanisms. Eur J Ophthalmol. Jul-Aug;2012 22(4):654–660. [PubMed: 22139616]
56. Mukhopadhyay R, Holder GE, Moore AT, Webster AR. Unilateral retinitis pigmentosa occurring in an individual with a germline mutation in the RP1 gene. Arch Ophthalmol. Jul; 2011 129(7): 954–956. [PubMed: 21746989]

Biographies

Tharikarn Sujirakul, MD received her medical degree from Mahidol University, Thailand in 2004. She completed her ophthalmology residency and fellowship in Vitreoretinal surgery at Ramathibodi hospital, Mahidol University and recently completed a research fellowship in hereditary retinal disease, electrophysiology and medical retina from Edward S. Harkness Eye Institute, Columbia University and Vitreous-Retina-Macula Consultants of New York. Her current research interests include medical and hereditary retinal disease, retinal imaging techniques and electrophysiologic study of the retina.

Michael Lin is a fourth year medical student at Columbia University College of Physicians and Surgeons. He completed his undergraduate studies at Brown University with a degree in biochemistry. Currently, he is a student researcher in the laboratory of Dr. Stephen Tsang, where he studies the molecular biology of macular degeneration and assists with clinical studies on retinal degenerative diseases. He plans to apply for residency in ophthalmology and is always seeking more research opportunities.

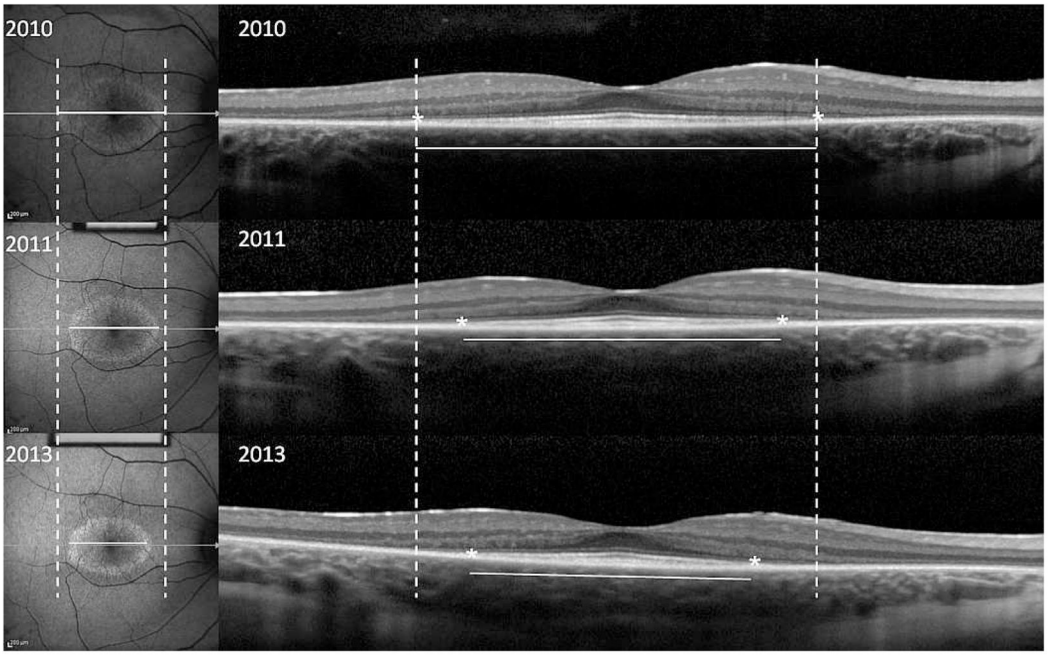

Figure 1. Structural measurements of a 13 year old girl with autosomal recessive retinitis pigmentosa (Usher's Syndrome)

Fundus autofluorescence (AF) images (left panels) and optical coherence tomography (OCT) images (right panels) monitor progression over time. Dashed lines indicate the initial width of the horizontal diameter of the hyperautofluorescent ring in the AF images, and the initial width of the ellipsoid zone line in the OCT images. Progressive constrictions of the horizontal diameter and ellipsoid zone line are shown by the shortening of the solid white lines measuring horizontal diameter and ellipsoid zone line width in the three annual visits.

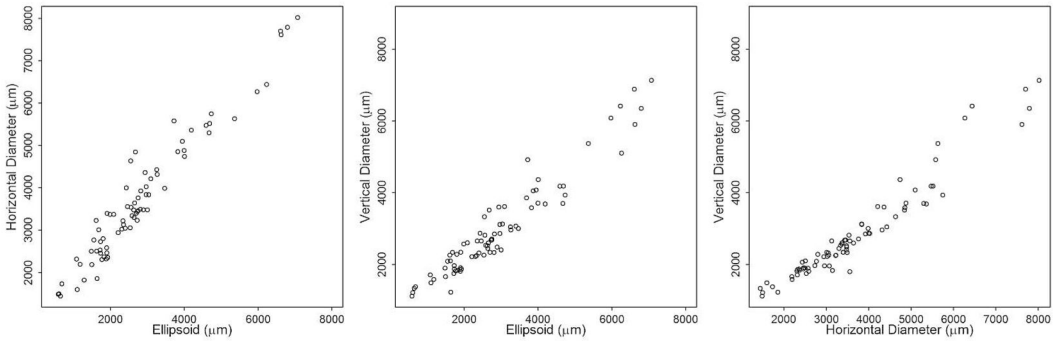

Figure 2. Correlation of standard-domain optical coherence tomography and fundus autofluorescence measurements in a cohort of 71 patients with retinitis pigmentosa

Scatterplots show AF horizontal ring diameter and SD-OCT ellipsoid zone width (left), AF vertical ring diameter and SD-OCT ellipsoid zone width (center), and AF vertical ring diameter and AF horizontal ring diameter (right).

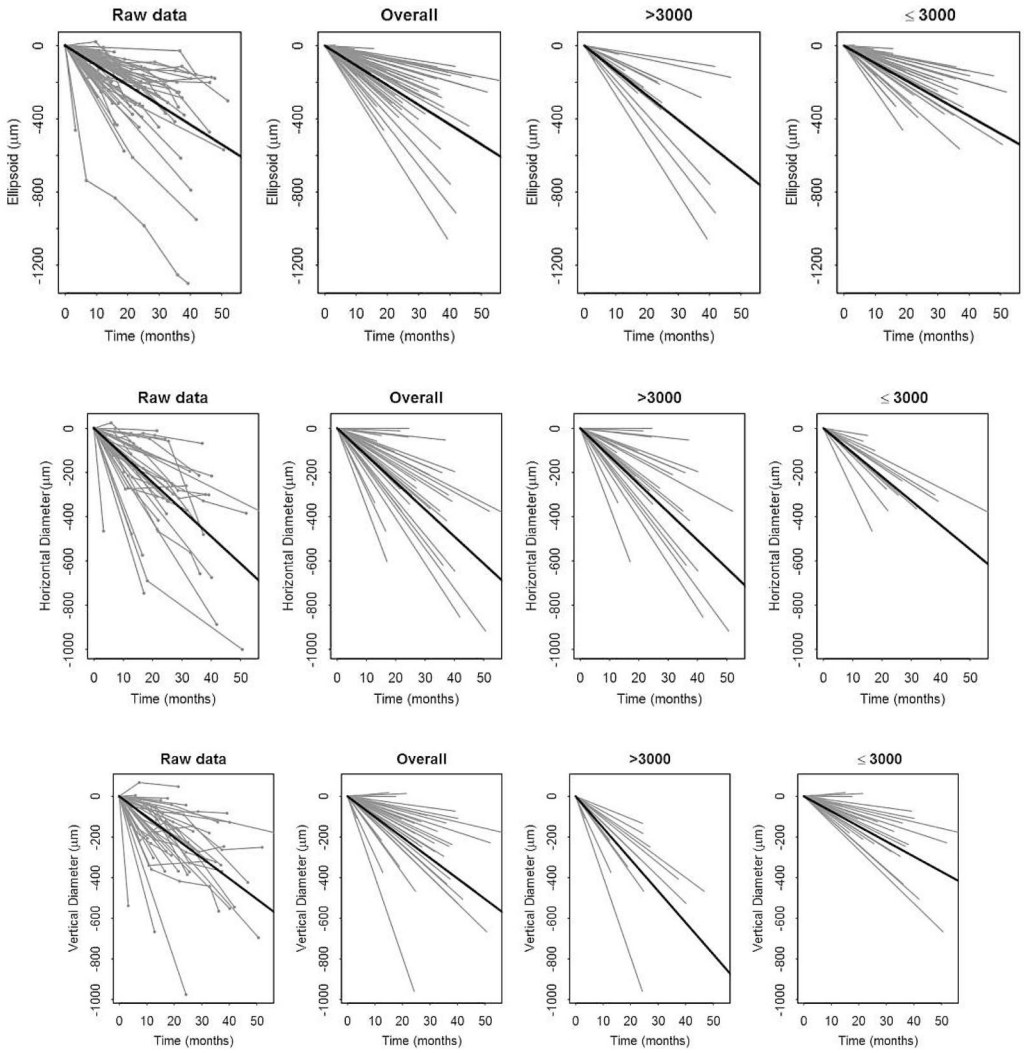

Figure 3. Structural progression of retinitis pigmentosa over the follow up period

Subjects have been centered to start at the same size to more clearly show the change over time. Changes over time for individual subjects are graphed as grey lines. In each row from left to right, the first panel graphs the raw data of individual subjects. The next 3 panels graph the random slopes from the mixed models. The third panel shows data from subjects with baseline size >3000; the fourth panel shows data from subjects with baseline size ≤3000. A solid line depicts the mean line of declination for the data of each graph.

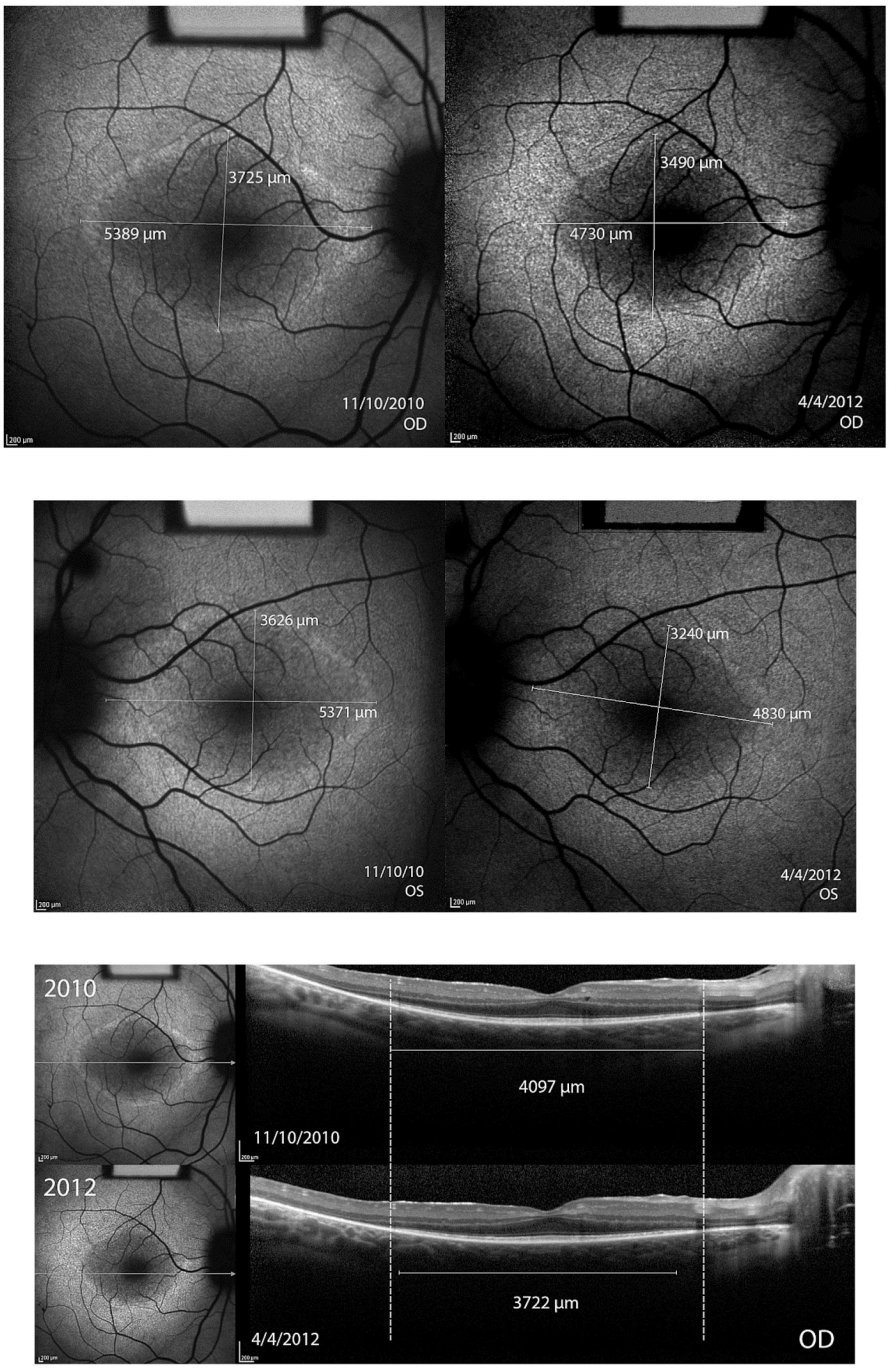

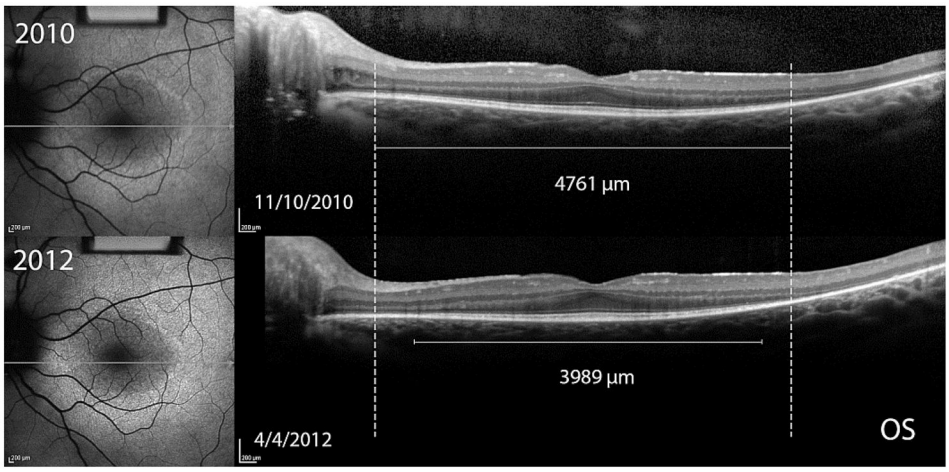

Figure 4. Asymmetry of structural progression in an 11 year old boy with X-linked retinitis pigmentosa

Dashed lines indicate the initial width of the ellipsoid zone line in the OCT images. Progressive constrictions of the ellipsoid zone line for OS and OD are shown by the shortening of the solid white lines measuring ellipsoid zone line width in the two visits 1.4 years apart. The difference between left and right eye progression using the mean of test and retest ellipsoid zone line measurements was 129.4µm/year. Fundus autofluorescence images of the hyperautofluorescent ring revealed a difference between eyes of 113.6µm/year using horizontal diameter measurements and 224.8µm/year using vertical diameter measurements.

Table 1

Characteristics of the 71 patients included in the study of progression in patients with retinitis pigmentosa using structural imaging

ID	Sex	Age	Mode of inheritance	Known Genotypes	Years of followup	Ellipsoid	Hyperautofluorescent ring	Comment
1	F	38	ARRP	PDE6A(p. Arg102Cys; p. Ser303Cys)	7.6	+		
2	F	80	ARRP	-	2.6	+	No residual ring	CME
3	F	13	ARRP	-	3.4	+	+	
4	F	80	ARRP	-	1.3	+	No residual ring	
5		26	ARRP	-	1.1	+	+	
6	F	24	ADRP	PRPF31(p.107_108del)	0.3	+	+	
7	F	22	ADRP	PRPF31(p.107_108del)	0.3	+		
8	M	18	ARRP	USH2A (p.Thr1238Arg:c.3713C>G, p.Cys3153STOP:c.9459C>A)	2.9	+	+	
9	M	73	ARRP	-	0.5	+	No residual ring	
10	F	56	ARRP	-	1.2	+	No residual ring	
11	M	51	ADRP	RHO (p.Asp190Asn)	3.3	+	+	
12	F	23	ARRP	USH2A (p.Glu478Asp); CNGB1 (c.3150delG p.Phe1051Leufs)	2.0	+	+	
12	M	17	ARRP	USH2A (p.Glu478Asp); CNGB1 (c.3150delG p.Phe1051Leufs)	2.0	+ beyond measurement	+	
14	M	75	ARRP	-	1.3	+	+	
15	F	23	ARRP	-	1.6	+	No residual ring	
16	M	54	ARRP	USH2A(p.Ser841Tyr,p.Tyr1992Cys)	1.8	Generalize granulated	+	
17	M	29	ARRP	-	3.5	+	+	CME
18	F	51	ARRP	-	2.9	+	+	CME
19	F	43	ADRP	-	2.3	+	+	
20	F	26	ARRP	-	0.5	Generalize granulated	+	
21	M	35	ADRP	-	2.9	+	No residual ring	
22	M	59	XLRP	-	0.7	+	+	
23	M	57	ADRP	CRX (p.Gly122Asp); PRPF31 (p.107_108del); MYO7A (p.Val411Ala)	2.9	+	+	CME
24	M	58	ARRP	-	2.5	+	No residual ring	
25	F	58	ARRP	-	0.3	+	+	
26	M	49	ARRP	-	1.3	+	No residual ring	
27	M	26	ADRP	-	3.3	+	+	
28	M	54	ADRP	RPE65 (p.Ala132Thr)	3.8	+	No residual ring	

ID	Sex	Age	Mode of inheritance	Known Genotypes	Years of followup	Ellipsoid	Hyperautofluorescent ring	Comment
29	F	25	ADRP	-	3.3	+	+	
30	M	27	ADRP	-	0.9	+	No residual ring	CME
31	M	32	ARRP	-	2.0	+	+	
32	M	62	ADRP	-	1.1	+	+	
33	M	80	ADRP	RPE65 (p.Ala132Thr)	3.8	+	No visible ring	
34	F	27	ARRP	-	1.5	+	No residual ring	
35	M	58	ARRP	-	3.3	+	No visible ring	
36	M	44	ARRP	-	2.2	+	+	CME
37	M	75	ARRP	-	3.0	+	No residual ring	
38	F	16	ADRP	RHO (c.937-27_-19delCCCTGACTC)	1.5	+	+	
39	F	35	ARRP	-	0.3			
40	F	58	ARRP	-	0.9	+	No visible ring	
41	M	46	ARRP	-	3.4	+	No visible ring	
42	M	21	ARRP	CRB1(p.Asp1005Val:c.3014A>T and p.Cys163Gly:c.487T>G)	0.6	+	Ring absent	
43	M	30	ARRP	-	3.8	+	+ Arc like OD	
44	F	30	ARRP	-	3.1	+	+	
45	F	25	ARRP	RGR (p.Ser66Arg); USH2A (p.Val2562Ala)	4.0	+	No residual ring	
46	F	41	ARRP	-	1.8	+	+	
47	M	31	ARRP	-c.8442_8443insT (novel frameshift mutation and p.Arg334Trp:c. 1000C>TC)	4.2	+	+	
48	M	45	ARRP	USH2A (c.8442_8443insT; p.Arg334Trp: c.1000C>TC	0.8	+	+	
49	M	19	ARRP	VLGR1(Gln2301stop: c.6901C>T and c.17455-2A)	4.3	+	+	
50	F	35	ADRP	PRPF31 (c.420+6C>T); SAG (p.Cys147Phe:c.440G>T); PROM1 (p.Ser290Arg: c.868A>C)	1.3	+	No residual ring	
51	F	55	ARRP	-	1.8	+	No residual ring	
52	F	12	ARRP	-	2.1	+	+	
53	M	12	XLRP	RPGR (c.202G>A)	1.8	+	+	
54	M	66	ARRP	-	2.6	+	+	
55	M	38	ARRP	-	1.0	+	+	
56	F	16	ADRP	PRPF31 (c.383T>A p.Leu128stop)	1.6	+	+	CME
57	F	37	ARRP	-	1.0	+	+	
58	F	72	ARRP	-	2.0	+	No residual ring	

ID	Sex	Age	Mode of inheritance	Known Genotypes	Years of followup	Ellipsoid	Hyperautofluorescent ring	Comment
59	M	41	ADRP	-	1.1	+	+	
60	M	58	ARRP	-	2.0	+	+	
61	M	30	XLRP	RPGR (c.2194del p.Glu732ArgfsX83)	1.5	+	+	
62	M	26	ADRP	RP1 (c.2029C>T p.Arg677*)	3.1	+	+	
63	F	45	ADRP	-	1.9	+	Arc like OD	CME
64	M	11	XLRP	RPGR (c.1307G>A p.Gly436Asp)	1.4	+	+	
65	F	50	ARRP	-	1.3	+	+	
66	F	12	ADRP	MYH11 (p.Leu668Val; p.Val1317Met); MYOM1 (p.Glu247Lys; p.Arg1477Trp)	3.1	+	+	CME
67	F	62	ADRP	-	2.7	+	+	
68	M	69	ARRP	-	2.5	+	No visible ring	
69	M	13	ARRP	PDE6B(c.1923_1969ins6del47)	2.4	+	+	CME
70	M	20	ARRP	PDE6B(c.1923_1969ins6del47)	2.6	+	+	CME
71	M	25	ARRP	-	0.8	+	+	

Genotypes are presented according to OMIM (Online Mendelian Inheritance in Man) notation.

ARRP = autosomal recessive retinitis pigmentosa; ADRP = autosomal dominant retinitis pigmentosa; XLRP = X-linked recessive retinitis pigmentosa; CME = cystoid macular edema

Table 2

Descriptive statistics of the difference between test and retest measurements for structural imaging parameters used to monitor retinitis pigmentosa progression

	Mean ± SD	Median	Lower quartile	Upper quartile	95th percentile
Ellipsoid zone width	80.7 ±84.3	53.5	22.0	112.5	243.8
Horizontal Diameter	99.5 ±120.4	63.5	30.0	116.0	296.3
Vertical Diameter	87.2 ±116.8	60.0	25.2	110.8	245.2

All units are in μm.

Table 3

Estimated proportion of patients with advanced stage retinitis pigmentosa exhibiting significant progression using structural measurements.

Years of Followup	1	1.5	2	2.5	3	3.5
ellipsoid zone line	0.37	0.60	0.73	0.81	0.91	0.96
horizontal diameter	0.48	0.69	0.81	0.83	0.83	0.83
vertical diameter	0.38	0.58	0.69	0.73	0.82	0.84

Best fit slopes from linear mixed models for each patient were projected over the indicated follow up times in years to determine the proportion of patients that exceeded the threshold of significant change, defined as the 75th percentile of test-retest measurement variability.

No patients were projected to have significant disease regression.

Table 4

The rate of progression in advanced stage retinitis pigmentosa calculated using standard domain-optical coherence tomography and fundus autofluorescence.

Outcome	Progression (Degree/year)	Progression (μm/year)	Standard error	p-value
Ellipsoid zone overall	0.45	130	11	<0.001
baseline <3,000 μm	0.40	115	12	<0.001
baseline ≥3,000 μm	0.57	163	19	0.04[a]
Horizontal diameter overall	0.52	147	15	<0.001
baseline <3,000 μm	0.46	131	28	<0.001
baseline ≥3,000 μm	0.53	152	20	0.6[a]
Vertical diameter overall	0.42	121	15	<0.001
baseline <3,000 μm	0.31	89	16	<0.001
baseline ≥3,000 μm	0.66	187	25	<0.001[a]

Ellipsoid zone line width was measured from standard domain-optical coherence tomography (SD-OCT) and the horizontal and vertical diameters of the hyperautofluorescent ring were measured from fundus autofluorescence (AF) imaging.

Subgroups according to baseline size greater than and less than 3000 μm were analyzed to determine whether the progression rate varied by baseline size.

[a]Note that here the p-values for the lines with baseline ≥3000 μm are for tests of the interaction terms.